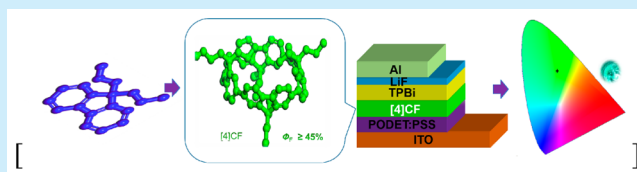


Synthesis and Crystal Structure of Highly Strained [4]Cyclofluorene: Green-Emitting Fluorophore

Yu-Yu Liu,^{||,†} Jin-Yi Lin,^{||,‡} Yi-Fan Bo,[†] Ling-Hai Xie,^{*,†} Ming-Dong Yi,[†] Xin-Wen Zhang,[†] Hong-Mei Zhang,[†] Teck-Peng Loh,^{*,§} and Wei Huang^{*,†,‡}[†]Key Laboratory for Organic Electronics and Information Displays & Institute of Advanced Materials (IAM), Jiangsu National Synergetic Innovation Center for Advanced Materials (SICAM), Nanjing University of Posts & Telecommunications, 9 Wenyuan Road, Nanjing 210023, China[‡]Key Laboratory of Flexible Electronics (KLOFE) & Institute of Advanced Materials (IAM), Jiangsu National Synergetic Innovation Center for Advanced Materials (SICAM), Nanjing Tech University (NanjingTech), 30 South Puzhu Road, Nanjing 211816, China[§]Division of Chemistry and Biological Chemistry, School of Physical and Mathematical Sciences, Nanyang Technological University, Singapore 637371, Singapore

Supporting Information

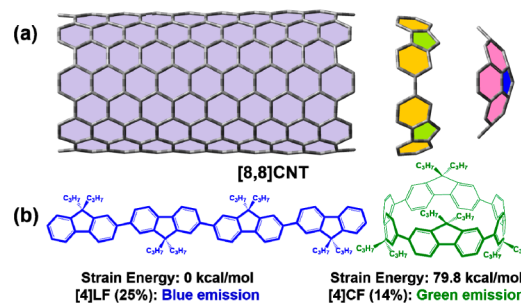
ABSTRACT: [4]Cyclo-9,9-dipropyl-2,7-fluorene ([4]CF) with the strain energy of 79.8 kcal/mol is synthesized in high quantum yield. Impressively, hoop-shaped [4]CF exhibits a green fluorescence emission around 512 nm offering a new explanation for the green band (g-band) in polyfluorenes. The solution-processed [4]CF-based organic light emitting diode (OLED) has also been fabricated with the a stronger green band emission. Strained semiconductors offer a promising approach to fabricating multifunctional optoelectronic materials in organic electronics and biomedicine.



Hoop-shaped cycloparaphenylenes (CPPs) and related π -conjugated molecules have attracted considerable attention from synthetic chemists and theoreticians owing to their aesthetic structure.¹ These strained molecules not only are used as elegant segments for nanotechnology,² host–guest molecules for supramolecular systems,³ ligands for metal coordination,⁴ and asymmetric inducer for catalysis chemistry⁵ but also exhibit novel size-dependent photophysical properties.⁶ Therefore, these series of molecules with radial p orbitals provide likely state-of-the-art strained semiconductor models to tune π -channels and optoelectronic properties in organic electronics. However, the low fluorescence quantum yield (Φ_F) of strained molecules with the high strain energy (>70 kcal/mol) restricts their application in OLEDs and organic lasers.^{1e,6b,7}

Different from the π -conjugated segments above, fluorene exhibits inherent larger exciton binding energies and excellent charge delocalization, enabling it to be an important building block in the molecular design of the light-emitting materials with high quantum yield.⁸ In this regard, fluorene-based strained molecules could achieve both merits of CPPs and fluorene-based emitters with high-efficiency feature, different from fluorene-based macrocycles⁹ with the same luminescence behaviors resembling linear oligofluorenes. Furthermore, it is noted that strained [n]cyclofluorenes ([n]CF) would offer a series of unprecedented models to obtain insight into the contribution of out-of-plane bending conformations to green band emission in polyfluorenes. In addition, [4]cyclo-2,7-fluorene is the key junction fragment to connect ring parts with bow-shaped end-caps in armchair CNTs (Scheme 1a). However, there are few

Scheme 1. (a) [4]CF Unit in CNT is Shown in Color; (b) Chemical Structure of [4]CF and [4]LF



reports on fully fluorene-based [n]CF.¹⁰ Herein, hoop-shaped [4]cyclo-9,9-dipropyl-2,7-fluorene ([4]CF, strain energy = 79.8 kcal/mol) as an example of strained semiconductors has been synthesized through another low toxicity method (Scheme 1).^{1b,i} The molecular structure of [4]CF has been first validated by X-ray crystallographic analysis. Contrary to the deep blue emission of controlled linear quaterfluorene ([4]LF), the [4]CF gives rise to stronger green emissions around 512 nm in the solution, film, and crystal state. Finally, the preliminary [4]CF-based nondoped OLED has been fabricated by solution-processed procedures.

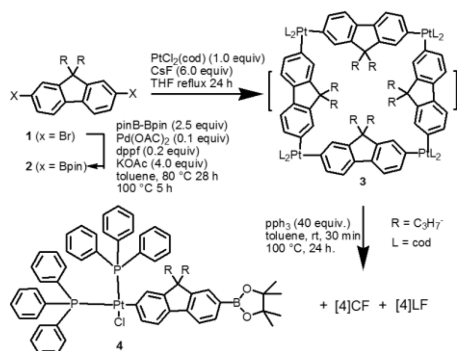
[4]CF can be synthesized according to the literature of CPPs which have been synthesized by four methods, such as Bertozzi

Received: October 31, 2015

Published: December 22, 2015

and Jasti's synthesis,^{1a,e,11} Itami's synthesis,¹² Yamago's synthesis,^{1b,i,13} and Ni⁰-mediated Stepien synthesis.¹¹ In this work, Yamago's method was chosen to prepare [4]CF via two steps utilizing a ligand exchange reaction and reductive elimination strategy.^{1b,i} The detailed synthetic route of the [4]CF is fully outlined in Scheme 2. Besides, a propyl group was

Scheme 2. Synthetic Routes of [4]CF and [4]LF



introduced as one of the alkyl groups at the 9-site of the fluorene segments to obtain suitable solubility. First, diboronic ester **2** was synthesized from dibromide **1** under Pd catalysis with a yield of 90%. **2** was heated with 1 equiv of PtCl₂(cod) (cod = 1,5-cyclooctadiene) and CsF in a refluxing tetrahydrofuran (THF) to give an intermediate of square shape tetranuclear Pt-complex **3** with the yield of 85%. Then the Pt-complex was treated with 40 equiv of PPh₃ in toluene at 100 °C for 24 h to afford [4]CF. The strain energy of [4]CF was estimated to be ~79.8 kcal/mol (Scheme S1), higher than that of [8]CPP (72.2 kcal/mol).¹⁴ Considering this point, the overall yield of [4]CF from the commercially available and inexpensive starting material **1** was reasonably high (14%). Besides, the linear quaterfluorene ([4]LF) can be obtained as a byproduct with an overall yield of 25%. Another yellow solid byproduct **4** was isolated. The structure of **4** was determined by using single-crystal X-ray analysis (Figure S10).¹⁵ Interestingly, [4]CF exhibits better solubility than CPPs in common organic solvents, such as cyclohexane, dichloromethane (CH₂Cl₂), chloroform (CHCl₃), THF, and toluene, which is important for application in solution-processed devices.

The ¹H NMR spectra of [4]CF, [4]LF, and the corresponding monomer **1** in CDCl₃ are shown in Figure 1. Two aromatic protons (H^b and H^c) are much further downfield (~7.57 and 7.51 ppm) than is observed in monomer **1**. However, the proton

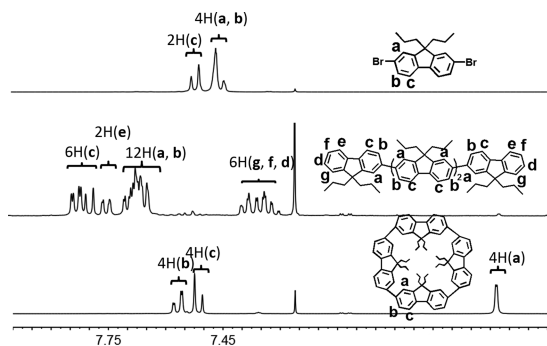


Figure 1. ¹H NMR spectra of [4]CF, [4]LF, and corresponding monomer in CDCl₃.

signal of H^a (~6.73 ppm) is shifted upfield by 0.71 ppm compared with that in dibromide **1**. Due to long-range coupling between H^a and H^b, the proton signal of H^b is split further into four peaks. [4]CF has been fully characterized by ¹³C NMR and high resolution (HR) mass spectrometry (MS) (see Supporting Information).

Single crystals of [4]CF suitable for X-ray analysis are obtained by the slow evaporation of THF solution at rt (Figure 2).

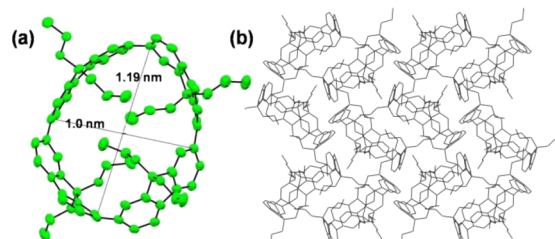


Figure 2. (a) X-ray diffraction crystallography of [4]CF. (b) Herringbone packing alignment of [4]CF.

Structure characterization by X-ray analysis reveals that [4]CF crystallizes in an achiral space group *Pna*2₁ at rt, which belongs to 10 polar point groups with the potential ferroelectric property,¹⁶ different from most reported [*n*]CPPs with the achiral space groups. Hoop-shaped [4]CF has an ellipsoidal cavity whose minor axes are 19% shorter than the major axes. This large deformation is probably due to steric hindrance associated with the propyl group. And, the average fluorenyl-fluorenyl dihedral angle for [4]CF is 34.60° lower than the calculated 38.90°. Compared to other fluorene-based semiconductors, the most arresting feature of [4]CF is out-of-plane distortion. The average distance between the 2 and 7 site (6.65 Å) in the fluorene is shorter than that in normal fluorene (6.80–6.90 Å).¹⁷ The tertiary carbons in each molecule are displaced out of the fluorene plane by an average of 28.93°. The bend angle (θ) of 57.86° is also calculated according to the previous works.¹⁸ To our knowledge, this conformation has the largest bend angle in fluorene systems. Besides, from the position of the H^a in the molecules, the upfield-shifted signals of H^a are probably due to the magnetic field produced by the ring currents of the fluorenyl π -system (Figure S9).¹¹ The analysis of the crystal packing structure indicates that the [4]CF can be self-organized into a herringbone formation in the presence of the CH \cdots π and π - π contacts from the *c* axis (Figure S11) and the tubular alignment from the *b* axis (Figure 2b). Impressively, the orientation of major axis helps to distinguish the array of the enantiomers in the crystal packing, which is probably induced by strain (Figure S12).¹⁹

The absorption and photoluminescence (PL) spectra of [4]CF in solution, and film are illustrated in Figure 3a. [4]CF in diluted solution exhibits a green color and has the maximum absorption at 349 nm (λ_{abs1}) and a shoulder-like absorption band at 398 nm (λ_{abs2}) with weak oscillator strength. [4]CF shows green photoluminescence with the emission maxima at 512 nm and two shoulder peaks at 396 and 416 nm. The UV absorption and PL spectra of [4]CF in toluene, CHCl₃, and DCE are similar to those in THF solution and film (Figure S14, Table S1). In addition, the concentration-dependent PL spectra of [4]CF in 1,2-dichloroethane (DCE) solution, normalized through the blue peak, are shown in Figure S15. The maximum emission at 512 nm is slightly changed with decreasing concentration from 10⁻⁴ to 10⁻⁹ M. The green index φ ($\varphi = I_{\text{green}}/I_{\text{blue}}$) increases

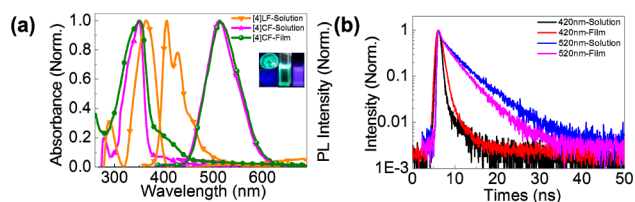


Figure 3. Optical properties of [4]CF and [4]LF. (a) UV and PL spectra of [4]CF and [4]LF in THF solution (10^{-5} M) and spin-coated film from CHCl_3 . (b) Transient decay spectra of [4]CF in THF solution (10^{-5} M) and spin-coated film from CHCl_3 .

with the concentration from 10^{-9} to 10^{-4} M. The shape of the PL spectrum of [4]CF in the crystal state is identical to that of other states (Figure S18). However, the emissions around 512 nm are not observed in the PL spectra of [4]LF in various states (Figure S19–S20).

To gain insight into the optical properties of [4]CF, time-dependent DFT calculations are carried out at the B3LYP/6-31G(d) level. According to calculation results (Scheme S2), the strongest absorption $\lambda_{\text{abs}1}$ at 349 nm can be assigned to a combination of HOMO \rightarrow LUMO+1 (2) and HOMO–1 (2) \rightarrow LUMO excitations. A weaker absorption $\lambda_{\text{abs}2}$ at 398 nm can be described as the forbidden transition involving HOMO and LUMO. Two emission bands at 396 and 416 nm for [4]CF can be assigned to the 0–0, 0–1 intrachain transitions.²⁰ And the maximum emission at 512 nm is assigned to the transition corresponding to the HOMO–LUMO energy with the oscillator strength (f) of 0.000. The structural relaxation from the Franck–Condon state^{6b} or the self-trapping of the lowest excitonic state due to electron–phonon coupling²¹ may induce the forbidden transition.

The quantum yield for [4]CF in solution and spin-coated film are estimated to be 0.45 and 0.48 (Figure 3b, Table S2), respectively, similar to [4]CFR.¹⁰ The values are higher than that of other hoop-shaped molecules with a similar ring size, such as [8]CPP (0.08^{6b} or 0.10⁷) and [4]cyclo-2,7-pyrenylene ([4]CPY) (0.05).^{4a} Further, the decay times of the blue emission band are found to be biexponential decay with lifetimes of 0.70 (80.81%) and 3.17 (19.19%) ns for [4]CF, 0.60 (79.22%) and 2.00 (20.78%) ns for [4]LF, respectively (Figure S21, Table S2). The decay time of the green emission for [4]CF exhibits single-exponential decay ($1A^*$) in dilute THF (7.7 ns) solution and film (10.4 ns) suggesting that only a single fluorescent species. In this regard, it is effectively concluded that the green emission at 512 nm is the intrinsic emitting property of [4]CF rather than the intra- and intermolecular charge-transfer induced by photo, interchain ketone-based excimers or fluorenone defects. Our result strongly indicated that the distorted conformation or entanglement chains of the fluorene segment probably induce green emission, resulting in the poor spectral stability in wide-band gap blue light-emitting polyfluorenes.⁸ The bending mode of chain would be the third mechanism of g-band formation after ketone and aggregates/excimers.

The oxidation curve is found to be reversible for [4]CF, indicating the stable radical cation intermediates. [4]CF has a lower half-wave oxidation potential of 0.61 eV (vs the ferrocene/ferrocenium couple) than [4]LF (0.88 eV) (Figures S22–23). The HOMO and LUMO energy levels of [4]CF are estimated to be about -5.35 and -2.35 eV from the above-mentioned experiments, respectively. The energy gap of [4]CF is calculated about 3.0 eV. Finally, the preliminary OLED using the [4]CF spin-coated film from CHCl_3 as an active layer has been

fabricated with a configuration of ITO/PODET:PSS (60 nm)/[4]CF (60 nm)/TPBi (40 nm)/LiF (1.2 nm)/Al (80 nm) (Figures S24–S25). And the electroluminescent (EL) spectra show the green emission at 508 nm with CIE coordinates of (0.25, 0.52) at the 5.38 V (turn-on voltage), similar to the corresponding PL spectra, suggesting single molecular emission in the film states (Figure 4). And OLED exhibits the maximum

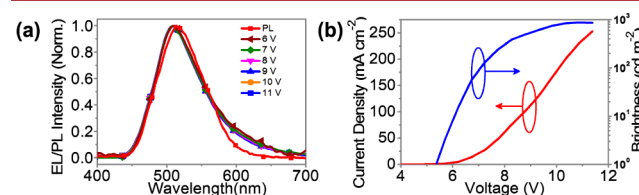


Figure 4. (a) Normalized EL spectra of devices at 6–11 V. (b) Current density–voltage–luminance characteristics of devices.

brightness of 878 cd/cm^2 at 10 V with a maximum luminescent efficiency of 0.83 cd/A , which is the first OLED via fluorene-based strained semiconductor used as the emissive material.

In conclusion, a fully fluorene-based strained semiconductor ([4]CF, strain energy = 79.8 kcal/mol) has been designed and synthesized successfully. Dramatically different from linear [4]LF, [4]CF showed a green emission at 512 nm with high-efficiency $\Phi_{\text{F}} \geq 45\%$. The bending conformation with a hoop shape not only became a tool for modulating the photoelectric properties of [4]CF but also offered an alternative explanation of the origin of the g-band in polyfluorenes for the first time. Furthermore, an OLED of a fluorene-based strained semiconductor has been fabricated via solution processing with a stronger green emission of 508 nm and CIE coordinates of (0.25, 0.52). Steric strain will be a potential tool to design multifunctional ferroelectric semiconductors for a wide range of memory applications in the future.

■ ASSOCIATED CONTENT

Supporting Information

The Supporting Information is available free of charge on the ACS Publications website at DOI: 10.1021/acs.orglett.5b03038.

Experimental details, compound characterization, and NMR spectra for all compounds (PDF)

■ AUTHOR INFORMATION

Corresponding Authors

*E-mail: iamlxie@njupt.edu.cn.

*E-mail: wei-huang@njtech.edu.cn.

*E-mail: teckpeng@ntu.edu.sg.

Author Contributions

¶Y.-Y.L. and J.-Y.L. contributed equally.

Notes

The authors declare no competing financial interest.

■ ACKNOWLEDGMENTS

This work was partially supported by the National Natural Science Funds for Excellent Young Scholar (21322402), National Natural Science Foundation of China (21504041, U1301243, 21274064, 51333007), National Key Basic Research Program of China (973) (2015CB932200), Doctoral Fund of Ministry of Education of China (20133223110007), Synergetic

Innovation Center for Organic Electronics and Information Displays, Natural Science Foundation of Jiangsu Province (BM2012010), Excellent science and technology innovation team of Jiangsu Higher Education Institutions (2013), and Open Project from State Key Laboratory of Supramolecular Structure and Materials at Jilin University (sklssm2015022). The project was funded by the Priority Academic Program Development of Jiangsu Higher Education Institutions and NUPTSF (NY214176). L.H.X. thanks Jiangsu Over-seas Research & Training Program for University Prominent Young & Middle-aged Teachers and Presidents.

REFERENCES

- (1) (a) Jasti, R.; Bhattacharjee, J.; Neaton, J. B.; Bertozzi, C. R. *J. Am. Chem. Soc.* **2008**, *130*, 17646–17647. (b) Omachi, H.; Segawa, Y.; Itami, K. *Acc. Chem. Res.* **2012**, *45*, 1378–1389. (c) Yamago, S.; Kayahara, E.; Iwamoto, T. *Chem. Rec.* **2014**, *14*, 84–100. (d) Lewis, S. E. *Chem. Soc. Rev.* **2015**, *44*, 2221–2304. (e) Golder, M. R.; Jasti, R. *Acc. Chem. Res.* **2015**, *48*, 557–566. (f) Darzi, E. R.; Jasti, R. *Chem. Soc. Rev.* **2015**, *44*, 6401–6410. (g) Yagi, A.; Segawa, Y.; Itami, K. *J. Am. Chem. Soc.* **2012**, *134*, 2962–2965. (h) Hitosugi, S.; Nakanishi, W.; Yamasaki, T.; Isobe, H. *Nat. Commun.* **2011**, *2*, 492. (i) Hitosugi, S.; Yamasaki, T.; Isobe, H. *J. Am. Chem. Soc.* **2012**, *134*, 12442–12445. (j) Iwamoto, T.; Kayahara, E.; Yasuda, N.; Suzuki, T.; Yamago, S. *Angew. Chem., Int. Ed.* **2014**, *53*, 6430–6434. (k) Ito, H.; Mitamura, Y.; Segawa, Y.; Itami, K. *Angew. Chem., Int. Ed.* **2015**, *54*, 159–163. (l) Mysliwiec, D.; Kondratowicz, M.; Lis, T.; Chmielewski, P. J.; Stepien, M. *J. Am. Chem. Soc.* **2015**, *137*, 1643–1649. (m) Patel, V. K.; Kayahara, E.; Yamago, S. *Chem. - Eur. J.* **2015**, *21*, 5742–5749. (n) Kayahara, E.; Patel, V. K.; Xia, J.; Jasti, R.; Yamago, S. *Synlett* **2015**, *26*, 1615. (o) Wong, B. M. *J. Phys. Chem. C* **2009**, *113*, 21921–21927.
- (2) Omachi, H.; Nakayama, T.; Takahashi, E.; Segawa, Y.; Itami, K. *Nat. Chem.* **2013**, *5*, 572–576.
- (3) (a) Iwamoto, T.; Watanabe, Y.; Sadahiro, T.; Haino, T.; Yamago, S. *Angew. Chem., Int. Ed.* **2011**, *50*, 8342–8344. (b) Iwamoto, T.; Watanabe, Y.; Takaya, H.; Haino, T.; Yasuda, N.; Yamago, S. *Chem. - Eur. J.* **2013**, *19*, 14061–14068. (c) Sato, S.; Yamasaki, T.; Isobe, H. *Proc. Natl. Acad. Sci. U. S. A.* **2014**, *111*, 8374–8379. (d) Hitosugi, S.; Ohkubo, K.; Iizuka, R.; Kawashima, Y.; Nakamura, K.; Sato, S.; Kono, H.; Fukuzumi, S.; Isobe, H. *Org. Lett.* **2014**, *16*, 3352–3355. (e) Iwamoto, T.; Slanina, Z.; Mizorogi, N.; Guo, J.; Akasaka, T.; Nagase, S.; Takaya, H.; Yasuda, N.; Kato, T.; Yamago, S. *Chem. - Eur. J.* **2014**, *20*, 14403–14409. (f) Ueno, H.; Nishihara, T.; Segawa, Y.; Itami, K. *Angew. Chem., Int. Ed.* **2015**, *54*, 3707–3711.
- (4) (a) Zabula, A. V.; Filatov, A. S.; Xia, J.; Jasti, R.; Petrukhina, M. A. *Angew. Chem., Int. Ed.* **2013**, *52*, 5033–5036. (b) Kubota, N.; Segawa, Y.; Itami, K. *J. Am. Chem. Soc.* **2015**, *137*, 1356–1361. (c) Kayahara, E.; Patel, V. K.; Mercier, A.; Kündig, E. P.; Yamago, S. *Angew. Chem., Int. Ed.* **2015**, Early view.
- (5) Hitosugi, S.; Matsumoto, A.; Kaimori, Y.; Iizuka, R.; Soai, K.; Isobe, H. *Org. Lett.* **2014**, *16*, 645–647.
- (6) (a) Iwamoto, T.; Watanabe, Y.; Sakamoto, Y.; Suzuki, T.; Yamago, S. *J. Am. Chem. Soc.* **2011**, *133*, 8354–8361. (b) Fujitsuka, M.; Cho, D. W.; Iwamoto, T.; Yamago, S.; Majima, T. *Phys. Chem. Chem. Phys.* **2012**, *14*, 14585–14588. (c) Segawa, Y.; Fukazawa, A.; Matsuura, S.; Omachi, H.; Yamaguchi, S.; Irle, S.; Itami, K. *Org. Biomol. Chem.* **2012**, *10*, 5979–5984. (d) Chen, H.; Golder, M. R.; Wang, F.; Jasti, R.; Swan, A. K. *Carbon* **2014**, *67*, 203–213. (e) Alvarez, M. P.; Burrezo, P. M.; Kertesz, M.; Iwamoto, T.; Yamago, S.; Xia, J.; Jasti, R.; Navarrete, J. T. L.; Taravillo, M.; Baonza, V. G. *Angew. Chem.* **2014**, *126*, 7153. (f) Chen, H.; Golder, M. R.; Wang, F.; Doorn, S. K.; Jasti, R.; Tretiak, S.; Swan, A. K. *J. Phys. Chem. C* **2015**, *119*, 2879–2887.
- (7) Darzi, E. R.; Sisto, T. J.; Jasti, R. *J. Org. Chem.* **2012**, *77*, 6624–6628.
- (8) (a) Xie, L. H.; Yin, C. R.; Lai, W. Y.; Fan, Q. L.; Huang, W. *Prog. Polym. Sci.* **2012**, *37*, 1192–1264. (b) Wang, L.; Zhang, G.-W.; Ou, C.-J.; Xie, L.-H.; Lin, J.-Y.; Liu, Y.-Y.; Huang, W. *Org. Lett.* **2014**, *16*, 1748–1751.
- (9) (a) Simon, S. C.; Schmaltz, B.; Rouhanipour, A.; Raeder, H. J.; Muellen, K. *Adv. Mater.* **2009**, *21*, 83–85. (b) Fomina, N.; Hogen-Esch, T. E. *Macromolecules* **2008**, *41*, 3765–3768.
- (10) Kayahara, E.; Rui, Q.; Kojima, M.; Iwamoto, T.; Suzuki, T.; Yamago, S. *Chem. - Eur. J.* **2015**, *21*, 18939.
- (11) Evans, P. J.; Darzi, E. R.; Jasti, R. *Nat. Chem.* **2014**, *6*, 404–408.
- (12) Takaba, H.; Omachi, H.; Yamamoto, Y.; Bouffard, J.; Itami, K. *Angew. Chem., Int. Ed.* **2009**, *48*, 6112–6116.
- (13) Yamago, S.; Watanabe, Y.; Iwamoto, T. *Angew. Chem., Int. Ed.* **2010**, *49*, 757–759.
- (14) Segawa, Y.; Omachi, H.; Itami, K. *Org. Lett.* **2010**, *12*, 2262–2265.
- (15) CCDC 1031897 (4) contains the supplementary crystallographic data for this paper. The data can be obtained free of charge from The Cambridge Crystallographic Data Centre via www.ccdc.cam.ac.uk/data_request/cif. See the Supporting Information.
- (16) Zhang, W.; Ye, H. Y.; Xiong, R. G. *Coord. Chem. Rev.* **2009**, *253*, 2980–2997.
- (17) (a) Song, Y.; Xu, W.; Zhu, D. *Tetrahedron Lett.* **2010**, *51*, 4894–4897. (b) Xie, L. H.; Hou, X. Y.; Hua, Y. R.; Huang, Y. Q.; Zhao, B.-M.; Liu, F.; Peng, B.; Wei, W.; Huang, W. *Org. Lett.* **2007**, *9*, 1619–1622.
- (18) Bodwell, G. J.; Fleming, J. J.; Miller, D. O. *Tetrahedron* **2001**, *57*, 3577–3585.
- (19) Hitosugi, S.; Nakanishi, W.; Isobe, H. *Chem. - Asian J.* **2012**, *7*, 1550–1552.
- (20) Fukuda, M.; Sawada, K.; Yoshino, K. *J. Polym. Sci., Part A: Polym. Chem.* **1993**, *31*, 2465–2471.
- (21) Adamska, L.; Nayyar, I.; Chen, H.; Swan, A. K.; Oldani, N.; Fernandez-Alberti, S.; Golder, M. R.; Jasti, R.; Doorn, S. K.; Tretiak, S. *Nano Lett.* **2014**, *14*, 6539.